An Inline Hydro-Mechanical Transmission (i-HMT) with a Rotatable Valve Cam to Improve Efficiency

Perry Y. Li , Evan Sand , Zihao Chen , and Dani Putra

Dept. of Mechanical Engineering, Univ. of Minnesota, Minneapolis, MN55455, USA
E-mail: { lixxx099,sandx114,chen6991}@umn.edu, daniputra0123@gmail.com

Abstract

A hydro-mechanical transmission (HMT) is a continuously variable transmission (CVT) that transmits power both hydraulically and mechanically, resulting in higher efficiencies than hydrostatic transmissions. While typical HMTs require a parallel mechanical transmission consisting of planetary and coupling gears, the inline configuration of the HMT (i-HMT), with a two-shafted pump, eliminates the need for such gearing making them less expensive, complex, and bulky. A potential drawback of the i-HMT is the compressibility-related throttling loss due to non-ideal valve timing. To reduce these losses and to improve efficiency, the concept of rotating the valve cam to adjust the valve timing for the different operating conditions is introduced. This paper focuses on the design, construction and testing of an experimental prototype. Experimental results comparing a stock eccentric cam and an optimized rotatable cam demonstrates that power efficiency can be improved by as much as 7% for a broad range of operating conditions.

Keywords: Hydromechanical transmission, pre-compression, de-compression, valve timing, valve cam.

1 INTRODUCTION

A hydro-mechanical transmission (HMT), like hydrostatic transmissions (HST), can vary its transmission ratio continuously. Traditional parallel HMT architectures, such as the output-coupled HMTs in Fig. 1-top, consist of a pair of hydrostatic pump/motors in parallel with a set of mechanical coupling and planetary gears. Since a portion of the power is transmitted via the more efficient mechanical path, an HMT is more efficient than a HST [1].

The large sizes and high costs associated with parallel HMTs are major barriers to their use. The Hondamatic (see e.g. [3]), shown in Fig. 1-bottom and Fig. 2, is an alternate, inline implementation of the HMT. Since planetary and coupling gears are not required, the inline HMT (i-HMT) is smaller and less complex. The Hondamatic transmission has been deployed in some commercial all-terrain vehicles (ATVs) since the 2000's. The i-HMT consists of:

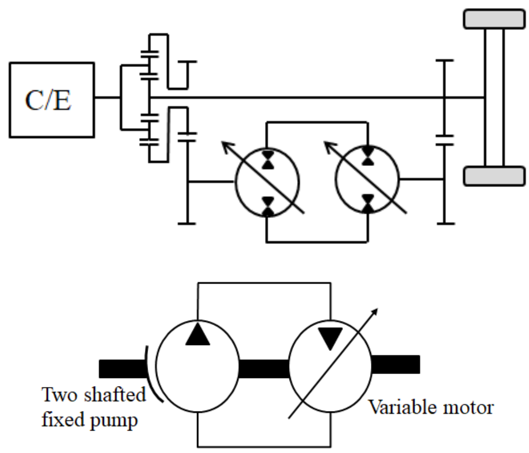

Figure 1: Schematics of Output-coupled HMT. Top: Traditional implementation [2]; Bottom: In-line implementation.

1. A rotatable wobble plate (labeled as shoe plate in Fig. 2) acting as the input for the pump.
2. Opposing axial piston pump and motor barrels fixed to a shared central shaft acting as the output.
3. A variable-angle motor swashplate that is rotationally fixed to the transmission case.
4. A system of radial distributor valves and valve cams connecting the pump and motor cylinders hydrostatically to high-pressure and low-pressure rings. The valve cam for the pump rotates with the wobble plate and pump housing; the one for the motor is fixed.

The wobble plate of the pump is the mechanical input, and the shared central shaft is the output shaft. The two-shafted pump (as the wobble plate and barrels can rotate independently) splits power between the mechanical and hydraulic channels, assuming the role of a $1:1:1$ planetary gear set on the left side of Fig. 1-top. Therefore, the Hondamatic i-HMT is an output-coupled input-split HMT.

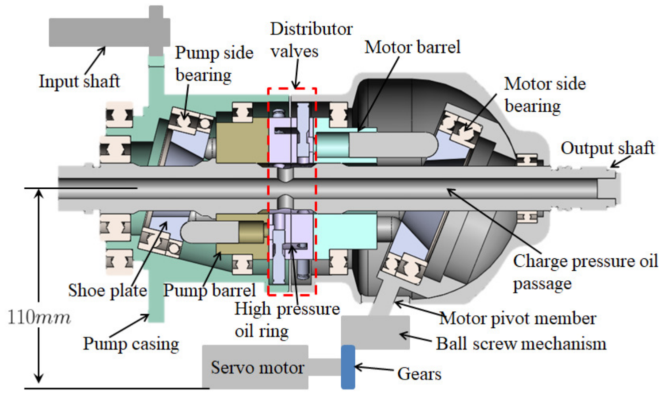

Figure 2: Cross-section view of the stock Hondamatic i-HMT [2].

From Fig. 1-b, using the fact that pump speed is the relative speed between the wobble plate (input shaft) and the barrel (output shaft), and flow continuity between the pump and motor, the ideal transmission ratio can be derived as:

$$i_{ideal} = \frac{\omega_{in}}{\omega_{out}} = \frac{T_{out}}{T_{in}} = \frac{D_p + D_m(t)}{D_p} \tag{1}$$

where ω_{in} and ω_{out} are the input and output shaft speeds, T_{in} and T_{out} are the input and output torques, D_p is the fixed pump displacement and $D_m(t)$ is the variable motor displacement. As $D_p \approx 6cc$ and $D_m(t) \in [0, 18cc]$, $i_{ideal} \in [1,4]$. When $D_m(t) = 0$, $i_{ideal} = 1$ as the transmission is locked up hydraulically. The input shaft, wobble plate, barrels of the pump and motor, and output shaft rotate as a rigid body. Power is transmitted purely mechanically. See [2] for a more detailed description and modeling of the functionality of the iHMT.

The performance of a stock Hondamatic i-HMT was experimentally evaluated in [2]. A possible power loss is throttling in the distributor valves due to the non-ideal fluid pre-compression and de-compression achieved with the stock eccentric circular valve cam. For instance, at zero motor displacement ($D_m = 0$), when the net motor flow is zero, the dead volumes in the motor piston chambers are repeatedly exposed to high and low pressures leading to wasteful repeated fluid compressions and de-compression cycles.

To address these compressibility losses, a second valve mode in which the motor piston chambers are closed to both high and low pressures was proposed in [4] specifically at lock up ($D_m = 0$). A rotatable valve cam concept was introduced as a secondary control input in [5] to vary the advance in valve timing. This approach applies to all motor displacements not just $D_m = 0$. The present paper describes the application of this latter concept to the Hondamatic - including the design, construction and experimental testing of a prototype.

The idea of rotating the port plate to adjust the displacements of piston machines has been proposed previously, e.g. recently in [6] and as a means of varying the transformation ratio of a hydraulic transformer [7]. The concept of using valve timing to control displacement is the premise of digital displacement machines in the partial stroke such as in [8, 9], typically using electric driven valves. This paper differs from these previous works in that the valve cam of the distributor valves is rotated in conjunction with a swash-plate to control both the displacement and the pre-compression.

The rest of the paper is organized as follows. Section 2 explains the valve timing in the stock Hondamatic i-HMT. In Section 3, the concept and the design of rotary cam are presented. Section 4 presents the cam design procedure. Section 5 presents the experimental test-stand and the testing procedures. Experimental results are presented in 6. Concluding remarks are presented in Section 7.

2 Valve Timing in the Stock i-HMT

The Hondamatic i-HMT uses a set of radial distributor valves instead of port plates to connect the piston chambers of the pump and the motor to high or low pressures (Fig. 3). When the radial spool valves move outwards, the piston chambers are exposed to the center low-pressure ring; and when the spool valves move inwards towards the center, the chambers are exposed to the high-pressure ring. The chambers are closed to both pressures in a small intermediate range of spool positions. As the radial valves rotate with the barrel, the distance between a fixed outer cam ring and the center of the rotating motor barrel determines the valve opening to the high or low pressure. In the stock Hondamatic, the cam is an eccentric circle, so the motor piston chambers are exposed to high pressure during the intake (motoring) half of the cycle and to low pressure during the exhaust half. The chambers are closed to both the high and low pressures prior to the top and bottom dead centers (TDC/BDC), presenting opportunities for pre-compression and de-compression.

Ideally, the decrease in fluid chamber volume during *pre-compression* would increase the fluid pressure from the low-pressure level during exhaust to exactly the high-pressure level when the valve is open to high-pressure. This would eliminate the throttling loss due to the pressure difference across the valve when it opens. Similarly, the increase in fluid chamber volume during *de-compression* would ideally decrease the fluid pressure from the high-pressure level during motoring to exactly the low-pressure level when the valve is open to low-pressure.

With the stock eccentric cam, the angles of the start and end of pre-compression (θ_{ps}, θ_{pe}) and de-compression (θ_{ds}, θ_{de}) are constant regardless of the pressure in the high-pressure ring or of the swashplate angle α_{sw}. The volume change during pre-compression and de-compression are:

$$\Delta V_p = \frac{A_p D}{2} \tan(\alpha_{sw}) \cdot (\cos(\theta_{ps}) - \cos(\theta_{pe})) \tag{2}$$

$$\Delta V_d = \frac{A_p D}{2} \tan(\alpha_{sw}) \cdot (\cos(\theta_{de}) - \cos(\theta_{ds})) \tag{3}$$

where α_{sw} is the swashplate angle, A_p and D are the piston area and the pitch cylinder diameter respectively. With the stock cam, $\theta_{pe} = 0°$ and $\theta_{de} = 180°$.

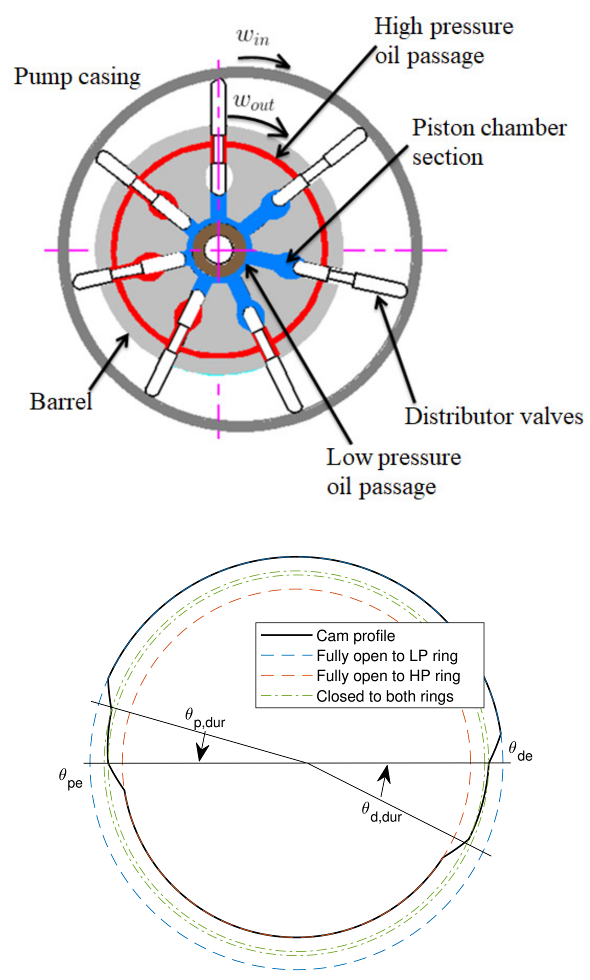

Figure 3: Top: (Exaggerated) Schematic of the stock eccentric cam profile; Bottom: Conceptual (non-circular) cam profile incorporating pre-compression and de-compression ($\theta_{pe} = 0$). Piston barrel is assumed to rotate counter-clockwise in bottom figure.)

On the other hand, the desired amount of volume change to avoid throttling depends on and increases with these quantities:

1. the dead volume in the piston chamber at the end of pre- and de-compression, given by:

$$V_{dead}(\theta_{pe}) = V_0 - \frac{A_p D}{2}\tan(\alpha_{sw})\cos(\theta_{pe}) \qquad (4)$$

   where V_0 is the dead-volume at zero swashplate angle ($\alpha_{sw} = 0$).

2. high-pressure level which in turn depends on input torque

3. compressibility of the fluid which depends on the amount of dissolved air content and pressure.

As these quantities change with the operating conditions of the transmission, the stock eccentric circular cam's fixed set of pre-compression and de-compression angles $\theta_{ps}, \theta_{pe}, \theta_{ds}, \theta_{de}$ cannot achieve the ideal pre-compression and de-compression for all pressures and motor displacements. In particular, as α_{sw} decreases, the dead-volume $V_{dead}(\theta_{pe})$ in (4) increases, thus requiring more volume change during pre-compression. However, the actual volume change ΔV_p in (2) provided by the fixed cam decreases (Fig. 4). The situation is slightly better for de-compression as both dead-volume and ΔV_d decrease.

3 Valve Timing Advance via a Rotatable Valve Cam

To cope with the varying required pre-compression and de-compression volume changes, an additional control degree-of-freedom is introduced by allowing the valve cam to rotate. Let the fixed pre-compression and de-compression durations as determined by a physical cam design be:

$$\theta_{p,dur} := \theta_{pe} - \theta_{ps} \qquad (5)$$
$$\theta_{d,dur} := \theta_{de} - \theta_{ds} \qquad (6)$$

By rotating the cam by $\Delta\theta(t)$ in the opposite direction of barrel rotation, valve opening and closing occur earlier so that:

$$\theta_{pe} = -\Delta\theta(t), \qquad \theta_{ps} = -\Delta\theta(t) - \theta_{p,dur}$$
$$\theta_{de} = -\Delta\theta(t) + 180^\circ, \quad \theta_{ds} = -\Delta\theta(t) + (180^\circ - \theta_{d,dur})$$

From (2)-(3), advancing the valve timing up to 90° increases the magnitude of the volume changes during pre-compression and de-compression ΔV_p and ΔV_d. The fluid volume to be pre-compressed is increased and the volume to be decompressed is reduced. In this way, the valve timing advance of $\Delta\theta(t)$ can be adjusted to be close to the optimal pre-compression and de-compression as the swashplate angle, high-pressure level, and fluid compressibility change.

In addition to its effect on ΔV_p and ΔV_d, advancing valve timing also decreases the effective displacement of the motor. It is because the motoring stroke is shortened as the high-pressure valve is closed prior to TBC, and the portion of the cycle prior to TDC is pumping instead of motoring, thus decreasing the net flow input from the high pressure over one cycle. Indeed, the effective fractional displacement relative to a motor in which the chamber is open to high-pressure between $0-180^\circ$ is:

$$\begin{aligned}\bar{D}_m(\alpha_{sw},\Delta\theta) &= \frac{\tan(\alpha_{sw})}{2\tan(\alpha_{sw,max})}\cdot[\cos(\theta_{pe}) - \cos(\theta_{ds})] \\ &= \frac{\tan(\alpha_{sw})}{2\tan(\alpha_{sw,max})}\cdot\left[\cos(\Delta\theta) + \cos(\Delta\theta + \theta_{d,dur})\right]\end{aligned} \qquad (7)$$

which shows that if $\Delta\theta > 0$, a larger swashplate angle α_{sw} is needed to maintain the same effective displacement when $\Delta\theta = 0$. Nevertheless, judicious combinations of α_{sw} and $\Delta\theta$ can achieve a range (albeit smaller) of desired motor displacements (hence i-HMT transmission ratios) while maintaining close-to-optimal pre-compression and de-compression.

With valve timing advance, the valves are open and closed as the pistons are moving. To minimize the throttling loss, the valves should be open and closed as quickly as possible.

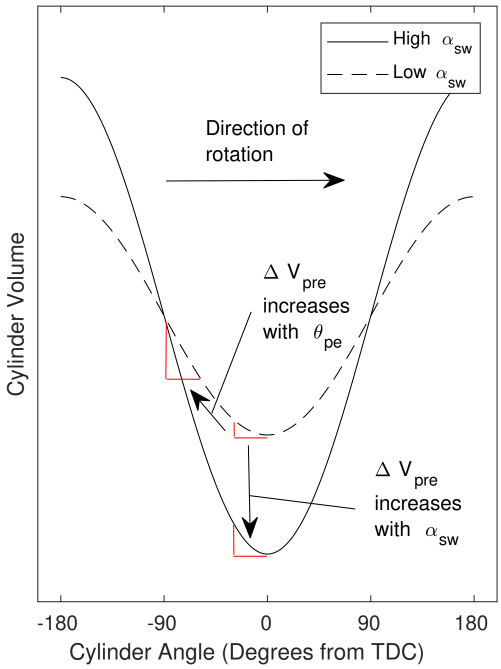

Figure 4: Effects of swashplate angle and cam angle on the change in cylinder volume during pre-compression: ΔV_{pre} increases with both $|\theta_{pe}|$ and α_{sw}.

This is achieved by the short transitions between valve opening and closing as illustrated in the cam profile in Fig. 3-bottom. The maximum rate is limited by the allowable pressure angle for the cam. In the stock eccentric circular cam, because the valves are open and close at TDC and BDC where the pistons are nearly stationary, the rate of valve opening is not as important.

4 Cam profile design

4.1 Design Strategy

For a given valve cam and operating pressure, settings for the cam angle θ_{pe} and swashplate angle α_{sw} may be chosen to achieve a prescribed motor displacement while exactly optimizing either pre-compression or de-compression but not both. A solution, suggested in [5], is to use passive check valves on the low-pressure side, at the expense of added complexity. Because of the effect of entrained air on the bulk modulus of the working fluid, the exact timing of pre-compression is more important: the bulk modulus of the working fluid is much lower at the end of de-compression (at low pressure) than at the end of pre-compression, so a non-optimal timing would not affect the cylinder pressure at the end of de-compression as much as it would affect the pressure at the end of pre-compression. For this reason, our strategy is, for a given cam profile (e.g. as specified by $\theta_{p,dur}$ and $\theta_{d,dur}$), to control the cam and swashplate angles to compensate for pre-compression while the cam profile is designed to minimizes throttling loss at the end of de-compression.

Based on this approach and the geometry of the motor, the optimal motor settings are calculated as in [5], but with the addition of:

1. Orifice leakage flows past the valve spool between the cylinder and both the high and low pressure rings
2. Laminar leakage through the piston-cylinder bore gap

Example relationships between the desired transmission ratio i_{ideal} and the cam timing advance angle $\Delta\theta$ and swashplate angle α_{sw} can be found in Fig. 11.

The analysis of pre-compression and de-compression requires a model of fluid compressibility. Our assumption is that the hydraulic fluid is a mixture of pure hydraulic oil with a constant bulk β and a fixed amount of entrained air that undergoes adiabatic compression/expansion. The volume fraction [1] α of the entrained air is assumed to be either 1% or 5% at atmospheric pressure.

Let p_h and p_t be absolute pressures in the high-pressure ring and in the tank, the optimal change in volume during pre-compression at full displacement is:

$$\Delta V_p = V_{dead}(\theta_{pe}) \cdot \left(\frac{1}{r_v} - 1\right) \tag{8}$$

where $V_{dead}(\theta_{pe})$ is the cylinder volume at the end of de-compression and r_v is the volume ratio of the working fluid between p_h and p_t:

$$r_v = \frac{e^{-(p_h - p_t)/\beta} + \alpha \left(\frac{p_h}{p_t}\right)^{-1/\gamma}}{1+\alpha} \tag{9}$$

where α is the volume fraction of the entrained air and $\gamma = 1.4$ is the polytropic index for the adiabatic process.

4.2 Optimization of Cam Parameters

To design the cam profile, it was first necessary to optimize the cam parameters $\theta_{p,dur}$ and $\theta_{d,dur}$, which are the angular durations of pre-compression and de-compression, respectively.

The motor settings are designed to compensate for pre-compression exactly for any operating condition. This causes valve-timing for de-compression to be non-optimal. Thus, the cam parameters are optimized to minimize the efficiency loss from non-optimal de-compression. To this end, an objective function was constructed which:

1. takes as inputs the cam parameters $\theta_{p,dur}$ and $\theta_{d,dur}$
2. iterates over the range of operating conditions possible with the test stand, and at each condition:
   (a) Prescribes motor settings to exactly optimize pre-compression
   (b) Evaluates the cylinder pressure at the end of de-compression using a model of pressure dynamics

[1] Ratio of air volume to pure liquid volume at low pressure

(c) Computes the resulting energy loss per cycle from non-optimal de-compression, using the principle of hydraulic effort [10]

(d) Computes the effect of the energy loss on efficiency "efficiency loss" by dividing by motor input power

(e) Adds a penalty if the pressure at the end of de-compression is below atmospheric pressure, or if the target transmission ratio tolerance cannot be achieved

3. Returns an average of the losses and penalties at all operating points for the cam parameters.

This objective function was then optimized using the `surrogateopt` function in MATLAB to find the cam parameters which would minimize the average impact of non-optimal de-compression on efficiency across all feasible operating conditions.

For $\alpha = 5\%$, the optimal parameters are: $\theta_{p,dur} = 5.82°$ and $\theta_{d,dur} = 10.89°$. Optimized cam parameters for $\alpha = 1\%$ were also obtained. Since testing for this case was limited, it will not be discussed.

4.3 Design of Cam Profile

Having selected the angular durations of pre-compression and de-compression, a spline profile was designed for the each cam. The following design constraints were used:

1. The profile must pass through the pre-compression and de-compression control points i.e. the valves must open and close to the HP and LP rings at the prescribed angles.

2. The pressure angle of the cam surface on the valve spools must not exceed 30°.

3. The valve spools must not separate from the cam surface at any operating condition.

4. The force at the cam-valve spool interface must not exceed 100 N at any operating condition.

Piecewise radial periodic cubic splines were used to design the profiles, using MATLAB's `perspline` function [11]. Control points were placed heuristically based on these constraints, and a resulting spline is shown in Fig. 5.

4.3.1 Cam Force Analysis

The forces at the cam-valve spool interface were evaluated to avoid excessive contact force and separation. The following forces were considered:

1. Inertial force of spool acceleration

2. Inner pressure of LP ring

3. Centrifugal force

4. Spikes in inward steady-state flow force on spool at the end of de-compression (the worst case for each speed)

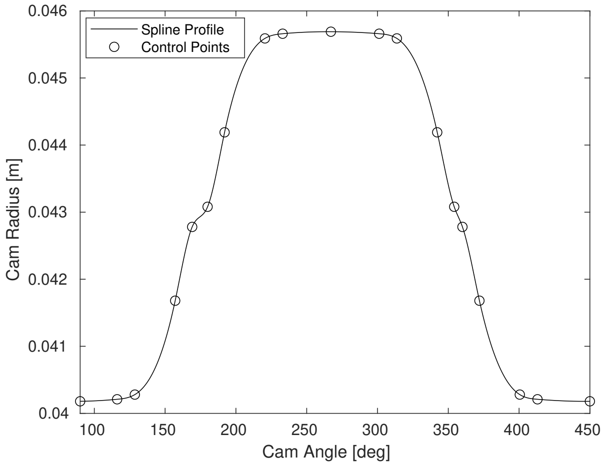

Figure 5: Cam radius as function of angle ($\alpha = 5\%$ case).

Contact force is a function of the motor speed and the cam angle. The contact force is between $19 - 39$ N for the stock cam and between $10 - 56$ N for the new cams across all operating conditions.

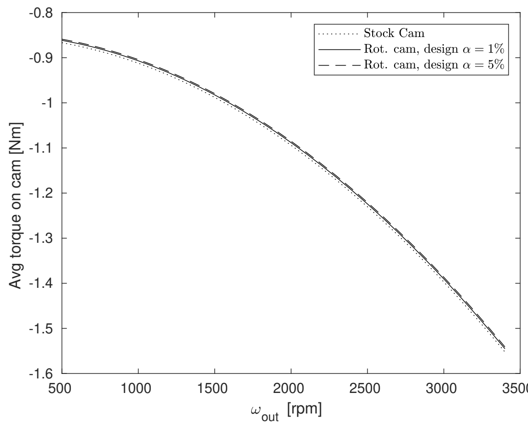

Figure 6: Torques from valve spools on cam for original cam and both rotatable cams, considering Coulomb friction and pressure angle effects.

4.3.2 Cam Torque Analysis

To verify that the torque applied to the new rotatable cams by the valve spools was not excessive, the torque was analyzed for both the stock cam and the new cams. The torque analysis considered torque from radial spool force based on pressure angle effects and Coulomb friction with $\mu = 0.12$. Torques from one spool were computed as functions of angle and motor speed, superimposed with an angle offset for all nine cylinders of the motor, and averaged over one rotation to find the average torque as a function of motor speed. As shown in Fig. 6, the magnitudes of torque for both rotatable cams are very slightly less than the torque on the original cam at all speeds. The torque did not exceed 2 Nm for any of the three cams. Based on this, it was determined that the effect of this torque on power loss was negligible, and that holding torque should

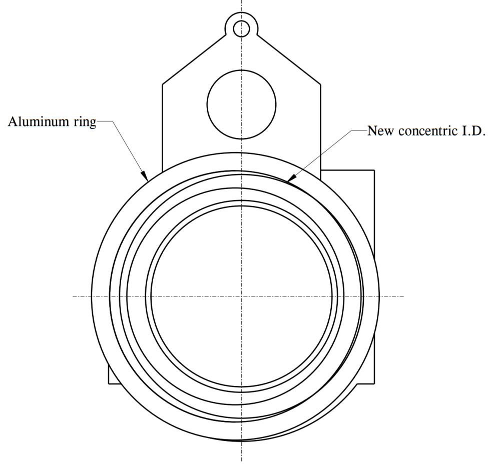

Figure 7: CAD model of modified motor case

not be a major concern in the actuation mechanism for cam rotation.

4.4 Mechanical Design

To design a method of actuating the rotatable cam in the assembled Hondamatic i-HMT in the test stand, a CAD model was created of the motor case based on physical measurements.

The stock motor case has an eccentric inner diameter which holds the circular cam ring. It was necessary to create a concentric inner diameter in the same place, in which the new cams could be rotated about the axis of the central shaft. A concentric cut could not be made without breaking through the case walls, so an aluminum ring was brazed onto the case before machining the concentric ID to match the wall thickness of the original motor case. The modified case is shown in Fig. 7.

To actuate the rotatable cams, an arm was designed to attach to the cams via a dowel and a threaded stud, passing through a slot in the motor case. The end of the actuation arm was fitted with a swiveling nut, which travels along a lead screw driven by a stepper motor. A photograph of the lead screw actuation is shown in Fig. 8. The motor swashplate was also actuated by a lead screw driven by a stepper motor, so the cam angle and swashplate angle could be adjusted together according to the prescribed operating conditions.

5 Experimental Testing

The mechanical input and output of the test stand used for performance testing were a pair of 28 cc Sauer/Danfoss S-42 variable-displacement hydrostatic pump/motors. They were connected in a regenerative configuration, meaning that the pump outlet was connected to the 20.68 MPa (3000 psi) high-pressure supply to re-capture the output power of the transmission. A 2.76 MPa (400 psi) charge pressure for the pump and motor was maintained using a pressure-reducing valve. The low-pressure ports of the hydrostatic pump/motors were kept at 2.76 MPa (400 psi) with a pilot-operated relief valve. A picture and a schematic of the test stand are shown in Fig. 9.

Inside the transmission case, the input shaft of the Hondamatic i-HMT is driven by gears with a 15:13 ratio as shown in Fig. 10. Charge fluid for the Hondamatic i-HMT was provided in a separate circuit (not shown in Fig. 9) by a small pump from the test stand case to the charge inlet. A constant 6.89 MPa (100 psi) charge pressure was maintained using a pressure-reducing valve.

These measurements were taken at the input/output shafts:

1. Input torque, with a Futek TRS300 torque cell on the input shaft
2. Input speed, with an RLS AM8192B magnetic encoder mounted on the input shaft
3. Output torque, with a Futek TRS300 torque cell on the input shaft
4. Output speed, with the S-42 pump's built-in encoder.

The input speed and output torque were regulated by adjusting the displacements of the test stand's hydrostatic motor/pumps at the input and output, respectively. Since only steady-state conditions are of interest, simple P-I controllers were used to regulate the input speed and the output torque.

As performance is sensitive to oil temperature, a temperature sensor was placed in the oil-sump to ensure that data were taken only when the temperature was between $35-40°C$.

Two stepper motors were used to adjust the cam and swashplate angles of the Hondamatic motor. Prior to performance testing, the optimal target angles were obtained by adjusting slightly from the analytical value to achieve the desired ratio more precisely and to improve on the efficiency. The changes are shown in Fig. 11-top. During testing, commands were given to two stepper motor controllers based on these modified settings. Because the stepper motors are undersized, the cam and swashplate angles were adjusted only when the transmission was at rest.

The test stand was operated in these ranges of conditions:

- Design entrained air content: 5%
- Input speed range: 1000-3000 rpm
- Output torque range: 10-100 Nm
- Target transmission ratio: 1 to 4
- Input power: 1 kW to 25 kW
- Operating pressure: 10 MPa to 50 MPa

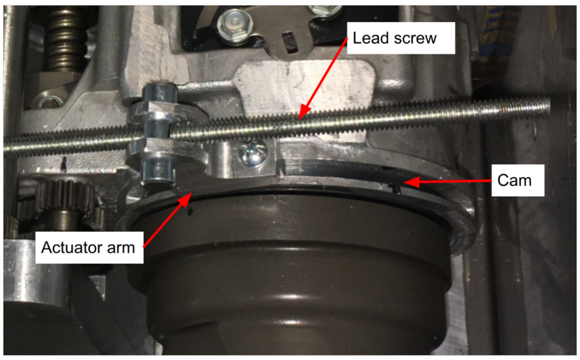

Figure 8: Lead screw actuation of rotatable cam.

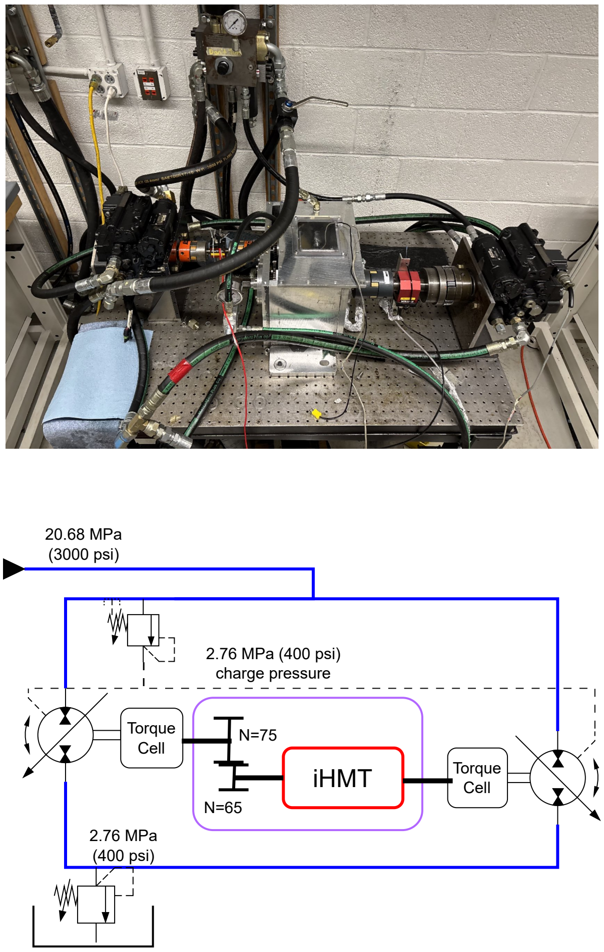

Figure 9: Picture and schematic of test stand used for performance testing.

At each condition, steady-state input and output torques and speeds were recorded and time-averaged to evaluate the achieved speed ratio and power efficiency. Sample input speed and output torque tracking performances are shown in Fig. 12.

6 Results

The efficiency (output power/input power) contours of the i-HMT with stock cam and the optimized 5% cam as functions of input speed and torque are shown in Fig. 13. The efficiencies between the stock and modified cams are directly compared in Figs. 14 and 15. Note that speed ratios in these figures correspond to the ratios between the input speed of the test stand (not of the iHMT) and the output speed. For both the stock and 5% cams, efficiency tends to be lower at low output torque and increases as output torque increases. The peak efficiencies achieved by the stock cam is about 75% whereas the 5% cam achieves a peak of about 80%. For both cams, the peak efficiency for ratio=1 is less than other ratios. When output torque is greater than or equal to 20Nm, the efficiency is higher with the modified cam than with the stock cam. Ignoring the exceptionally low efficiency of the stock cam at 40Nm and ratio = 1, the increase can be as much as 7% (absolute).

Comparing Figs. 14 and 15, it is apparent that at 1000-2000

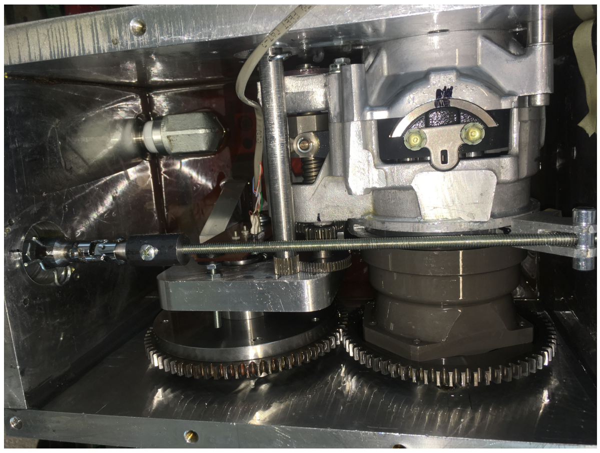

Figure 10: i-HMT inside the test stand transmission case.

RPM, the efficiencies of both cams do not vary with speeds significantly. This is confirmed in the surface plots in Fig. 16 where the efficiency surfaces at 1000 RPM and 2000 RPM are practically the same.

In Fig. 17, the efficiencies of both cams are plotted against input torque for all the data points. Whereas Figs. 14-15 and 16 show efficiency as a function of output torque and ratio, Fig. 17 indicates that efficiency is mainly a function of input torque. As input torque, input gear ratio (15:13), and system pressure $p_h - p_t$ (difference between high and low pressure) are directly related by:

$$T_{in} = \frac{13}{15}\frac{D_p}{2\pi}(p_h - p_t)$$

this suggests that efficiency is dictated mainly by the system pressure. In particular, efficiency is highest at about 30 Nm which corresponds to 27 MPa. The maximum working pressure of the Hondamatic is 50-60 MPa.

7 Conclusions

A rotatable valve cam with an optimized profile has been proposed as a method of reducing the compressibility losses in the variable displacement motor of an inline hydromechanical transmission (i-HMT). This introduces an additional control degree-of-freedom for adjusting the motor's valve timing to specifically control pre-compression at different operating conditions so as to avoid throttling losses due to unequal pressure when the valve opens. The approach has been reduced to design, prototyped and experimentally tested by modifying the valve cam of an stock Hondamatic i-HMT. Experimental results show that an optimized valve cam for oil with 5% entrained air does improve efficiency over the stock cam by as much as 7% over a broad range of operating conditions. Although this paper focuses on improving the efficiency of an i-HMT, it should be applicable to other axial piston machines as well.

References

[1] B. Carl, M. Ivantysynova, and K. Williams, "Comparison of operational characteristics in power split con-

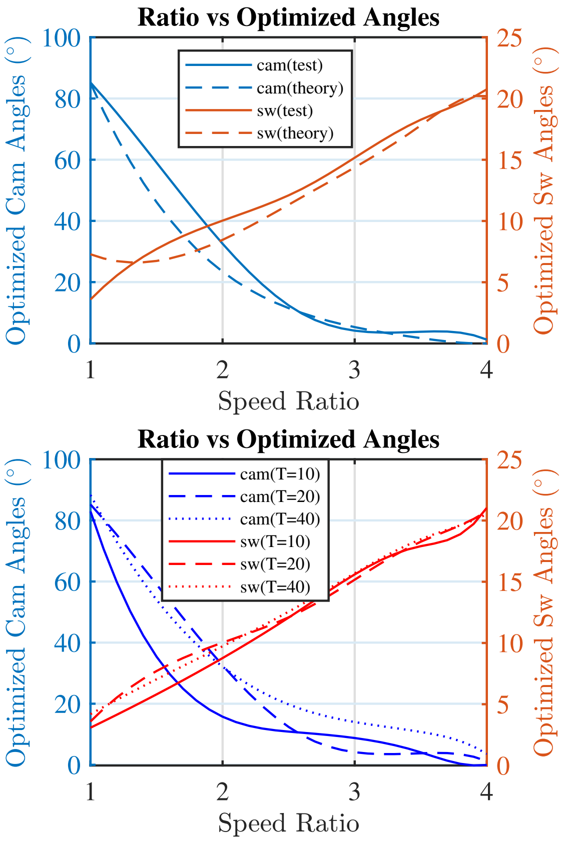

Figure 11: Optimal cam and swashplate angles for the 5% cam and 2000 RPM. Top) Analytical and optimized angles for $T_{out} = 20Nm$. Bottom) Optimized angles $T_{out} = 10Nm, 20Nm, 40Nm$.

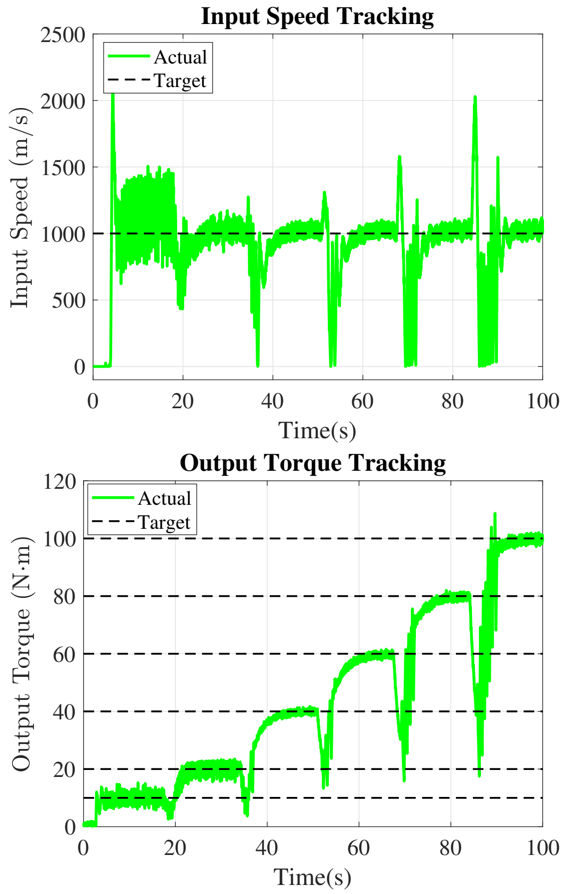

Figure 12: Sample input speed and output torque tracking results.

tinuously variable transmissions," *SAE Technical Paper Series - 2006-01-3468*, 2006.

[2] X. Hu, C. Jing, and P. Y. Li, "Modeling and experimental testing of the hondamatic inline hydro-mechanical transmission (iHMT)," *ASME J. of Dynamic Systems, Measurement, and Control*, vol. 142, no. 5, 2020.

[3] K. Nagatomo, "On hydro-mechanical hybrid transmission," in *Proceedings of the JFPS International Symposium on Fluid Power*, vol. 1993, pp. 273–278, The Japan Fluid Power System Society, 1993.

[4] J. Barkei and P. Y. Li, "Improving the efficiency of a compact inline hydro-mechanical transmission (iHMT) at lock-up," *Proc. of ASME/BATH 2021 Sym. on Fluid Power and Motion Control*, October 2021.

[5] E. D. Sand and P. Y. Li, "Incorporating a rotatable valve cam to improve the efficiency of a hydraulic motor in an inline hydro-mechanical transmission (i-HMT)," in *Proc. of Bath/ASME Sym. on Fluid Power and Motion Control*, vol. 86335, p. V001T01A029, 2022.

[6] L. Ericson, S. Kärnell, and M. Hochwallner, "Experimental investigation of a displacement-controlled hydrostatic pump/motorby means of rotating valve plate," in *The 15th Scandinavian Int. Conf. on Fluid Power, SICFP 17, Linköping, Sweden*, vol. 144, pp. 19–27, 2017.

[7] G. E. Vael, P. A. Achten, and Z. Fu, "The INNAS hydraulic transformer the key to the hydrostatic common pressure rail," in *SAE Tech. Paper*, 2000.

[8] M. Ehsan, W. Rampen, and S. Salter, "Modeling of digital-displacement pump-motors and their application as hydraulic drives for nonuniform loads," *J. Dyn. Sys., Meas., Control*, vol. 122, no. 1, pp. 210–215, 2000.

[9] M. B. Rannow, P. Y. Li, and T. R. Chase, "Discrete piston pump/motor using a mechanical rotary valve control mechanism," in *Proc. of the 8th workshop on digital fluid power, Tampere, Finland*, pp. 83–94, 2016.

[10] J. Barkei and P. Y. Li, "Hydraulic effort and the efficiencies of pump and motors with compressible fluid," *Proceedings of ASME/BATH 2020 Symposium on Fluid Power and Motion Control*, September 2020.

[11] J. Bastien, "Periodical cubic interpolation." `https://www.mathworks.com/matlabcentral/fileexchange/46580-periodical-cubic-interpolation`, May 2014.

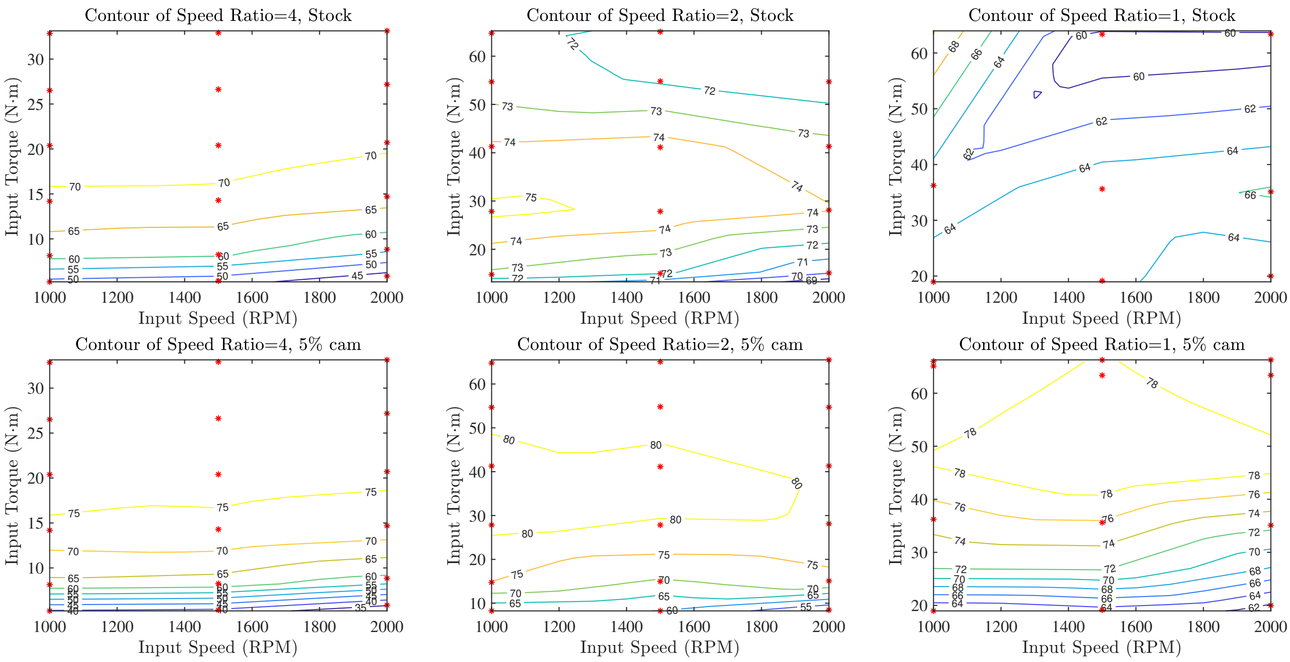

Figure 13: Efficiency of stock and 5% cam at ratio=4, 2, and 1

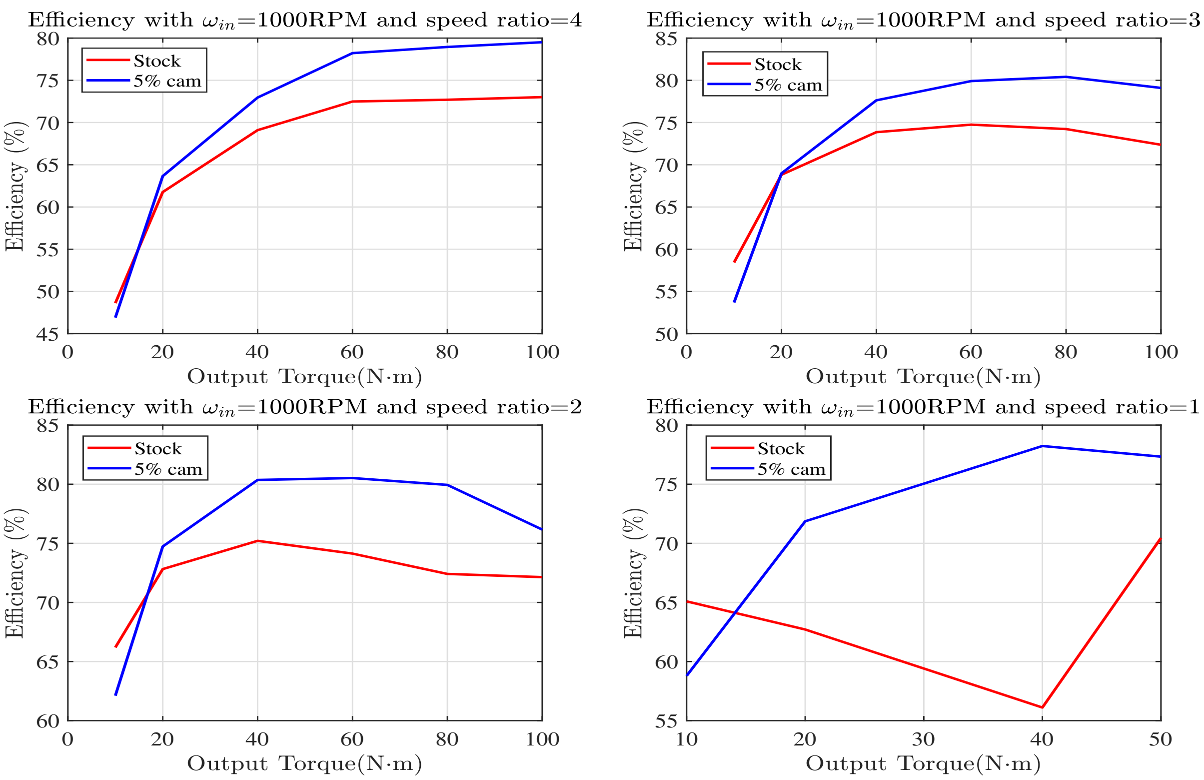

Figure 14: Efficiency of stock and 5% cams versus output torque at ratio = 4,3,2,1 and input speed = 1000 RPM.

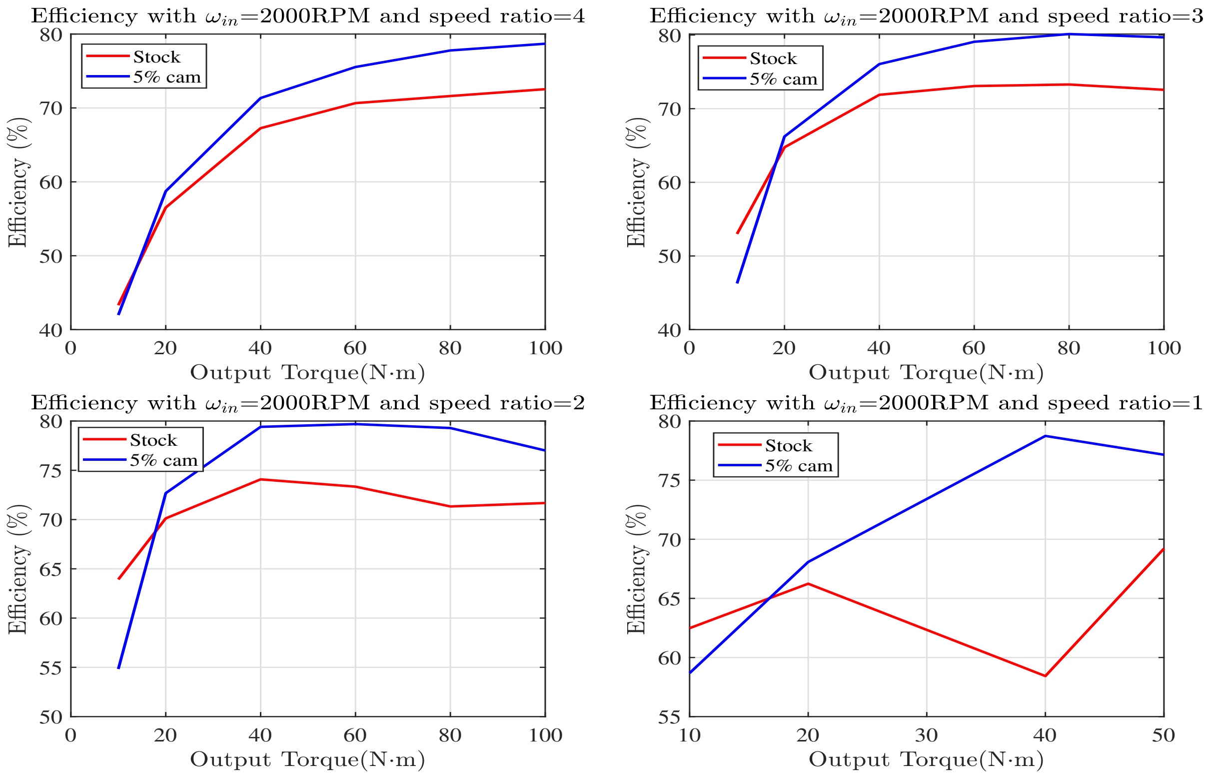

Figure 15: Efficiency of stock and 5% cams versus output torque at ratio = 4,3,2,1 and input speed = 2000 RPM.

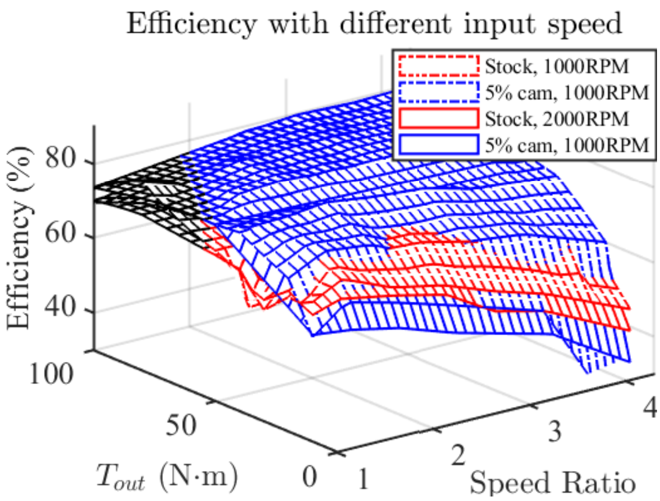

Figure 16: Efficiencies at different speeds.

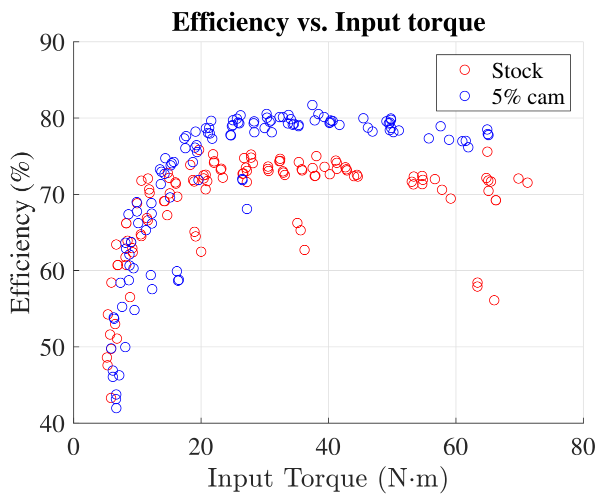

Figure 17: Efficiencies vs input torques (all cases).